Magic islands and barriers to attachment: A Si/Si(111)7×7 growth model

J. Myslivečekˆ* and T. Jarolímek
Department of Electronics and Vacuum Physics, Faculty of Mathematics and Physics, Charles University, V Holešovičkách 2, 180 00 Praha 8, Czech Republic

P. Šmilauer
Institute of Physics, Academy of Sciences of the Czech Republic, Cukrovarnická 10, 162 53 Praha 6, Czech Republic

B. Voigtländer and M. Kästner
Institut für Grenzflächenforschung und Vakuumphysik, Forschungszentrum Jülich, 52425 Jülich, Germany
(Received 26 April 1999; revised manuscript received 3 August 1999)

Surface reconstructions can drastically modify growth kinetics during initial stages of epitaxial growth as well as during the process of surface equilibration after termination of growth. We investigate the effect of activation barriers hindering attachment of material to existing islands on the density and size distribution of islands in a model of homoepitaxial growth on a Si(111)7×7 reconstructed surface. An unusual distribution of island sizes peaked around ''magic'' sizes and a steep dependence of the island density on the growth rate are observed. ''Magic'' islands (of a different shape as compared to those obtained during growth) are observed also during surface equilibration. [S0163-1829(99)08343-5]

Investigation of island structures formed during the initial stages of epitaxial growth allows us to explore kinetic mechanisms that govern the ordering of deposited atoms.[1] A lot of attention has recently focused on the time- and growth-conditions dependence of the island density[2] as well as on the bell-shaped distribution of island sizes[2] whose origin can be traced back to the distribution of island capture zones.[3] However, real growth systems are invariably more complicated than the idealized models of epitaxy commonly used. For example, the presence of surface reconstructions can completely change the growth behavior.

In homoepitaxy of Si on Si(111)7×7 reconstructed surface, a process of ''reconstruction destruction'' was described by Tochihara and Shimada.[4] The need to cancel surface reconstruction around a growing island gives rise to *barriers to attachment* of new material to existing islands. Growth with the barriers to attachment has been already studied theoretically: The dependence of the island density on growth conditions was explored using analytic methods,[5,6] while kinetic Monte Carlo (KMC) simulations of a simple growth model revealed an island-size distribution multiple peaked around ''magic'' sizes.[7]

In this paper, we present a detailed KMC model of Si/Si(111)7×7 molecular-beam epitaxy (MBE), with barriers to attachment included. With the help of this model, we investigate the time- and growth-rate dependence of the island density, the shape of the island-size distribution, as well as island decay and filling of vacancy islands on the surface. The results of our simulations compare favorably to available experimental data about the Si/Si(111)7×7 system. We also discuss those features of the model kinetics that are specific to growth with barriers to attachment.

Dynamics of Si/Si(111)7×7 MBE growth was experimentally studied by Voigtländer *et al.*[8–10] The most interesting feature observed, the existence of kinetically stabilized magic sizes in the island-size distribution, was reported and KMC modeled in Ref. 7. Another experiment[11] revealed a high scaling exponent $\chi \approx 0.75$ determined from

$$N \propto F^{\chi}, \tag{1}$$

the dependence of the island density N on the deposition rate F at constant temperature and amount of deposited material. The relaxation behavior of Si islands and vacancies on Si(111)7×7 surface was studied in Refs. 12–14. The temperature dependence of decay rates of a single adatom or vacancy island was determined.[12,13]

The model discussed in this work is a generalization of the model from Ref. 7. The model is based on the known structure of Si(111)7×7 reconstruction and the ''reconstruction destruction'' process proposed by Tochihara and Shimada.[4]

Si(111)7×7 surface bilayer is divided by dimer rows into half-unit cells (HUC's) of the 7×7 reconstruction. The half-unit cells differ in structure: In an unfaulted (U) HUC, the surface bilayer follows bulk bilayer stacking, whereas in a faulted (F) HUC, the bilayer is 30° rotated with respect to the bulk, forming a *stacking fault*. On top of each HUC, six Si adatoms are sitting.[15]

During Si growth on Si(111)7×7 surface, islands with reconstruction on top are formed. Silicon atoms arrive to the island edge and fill HUC's next to it. In order to become a part of the island, the reconstruction in the HUC must be dissolved, and the extra Si atoms has to be incorporated into Si bulk and form a new reconstructed surface. The reconstruction destruction is an activated process, and the barrier to attachment of material to an island is supposed to be higher in F-HUC's than in U-HUC's due to the need to remove the stacking fault.[4]

Experiments show that the mechanism of transport of Si atoms on Si(111)7×7 surface is very complicated.[16,17] Since in general the processes at island edges determine be-

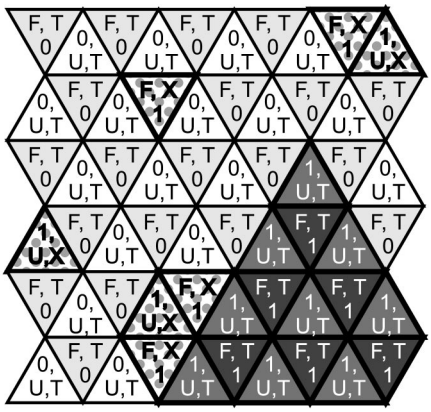

FIG. 1. The model: material units on a honeycomb lattice are assigned heights in BL Si(111), indicators of the presence of a stacking fault (F,U) and of material status (X,T). The units randomly walk on the surface and undergo transformation $X \rightarrow T$. Thereafter, they can detach from the island undergoing $T \rightarrow X$ transformation.

havior of growth models (as they determine the growth behavior of real systems), we decided to use a coarse-grained model that allows to model easily collective processes during ''reconstruction destruction'' around island edges. The simulation scheme ignores all processes on the length scales smaller than a HUC and on the time scales shorter than the time required to transport material from one HUC to its nearest neighbor.

In the model, material is deposited, diffuses, agglomerates, and transforms in units that represent HUC's of Si(111)7×7 reconstruction. Units are placed on a honeycomb lattice. Each site (HUC) in the model is assigned three parameters (Fig. 1): Height in bilayers of Si(111), an indicator of the presence of a stacking fault (F or U HUC's), and of material status (X or T HUC's). T (transformed) HUC represents the reconstructed surface of the substrate or of the island, X (untransformed) HUC represents Si atoms on the substrate that have not beeen incorporated into islands.[18] HUC's perform random walk with the hopping rate $\nu_D = \nu_0 \exp(-E_D/k_BT)$ where $E_D = E_S + (x+t)E_N^X$ for an X-HUC, $E_D = E_S + xE_N^X + tE_N^T$ for a T-HUC, x and t being the numbers of X and T neighbors, respectively, E_N^X the bond strengths of $X-X$ and $X-T$ pairs, E_N^T the bond strength of a $T-T$ pair, and E_S the surface barrier to diffusion. The rate of an X-HUC transformation is $\nu_T = \nu_0 \exp(-E_T/k_BT)$ where $E_T^F = E_A - tE_{\text{edge}}$ for an F-HUC, $E_T^U = E_A - tE_{\text{edge}} - E_{\text{diff}}$ for a U-HUC, E_A being the barrier to attachment, E_{edge} a decrease in the barrier due to a transformed neighbor, and E_{diff} the barrier difference for F- and U-HUC overgrowth. Transformation of an island begins at an F-HUC with $\geqslant 2$ X neighbors, and the rate of this nucleation process is $\nu = \nu_0 \exp[(E_T - E_{\text{edge}})/k_BT]$.

The model has seven parameters, here we report results for $\nu_0 = 10^{13}\ \text{s}^{-1}$, $E_S = 1.5$ eV, $E_N^T = 0.3$ eV, $E_N^X = 0.1$ eV, $E_A = 2.3$ eV, $E_{\text{edge}} = E_{\text{diff}} = 0.35$ eV, which gave the best agreement with experimental results. Using the model, we tried to reproduce both growth and equilibration processes on the Si/Si(111)7×7 surface on a real time and spatial scale. The HUC in the model is thus considered to be 1 bilayer (BL) of Si(111) thick, of a triangular shape with the edge length of $a = 26.9$ Å and consisting of 49 Si atoms. All calculations were performed on 200×200 HUC lattice with periodic boundary conditions.

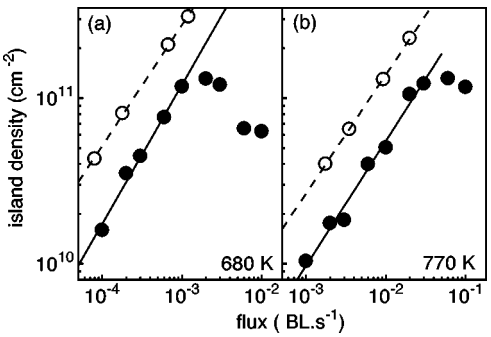

FIG. 2. Flux dependence of the island density N for Si/Si(111)7×7 MBE is $N \propto F^{\chi}$ with $\chi \approx 0.75$. Experimental (○) (Ref. 11) and modeled (●) $N(F)$ dependence for 680 K (a) and 770 K (b) are shown. In the model, N at $\Theta_{\text{tot}} = 0.15$ BL was measured.

Growth. In Si/Si(111)7×7 MBE, a relatively high scaling exponent χ [Eq. (1)] is observed. The experimental value of $\chi \approx 0.75$ for $T = 680$ and $T = 770$ K was reported in Ref. 11. In this experiment, samples were prepared at a given temperature by deposition of ≈0.15 BL Si on the Si(111)7×7 surface followed by rapid quenching to room temperature. The experimental morphologies of the layer can therefore be considered snapshots of the Si/Si(111)7×7 surface morphology evolution.

In the model, we calculated the flux dependence of the density of *transformed* (i.e., crystalline) islands N at constant *total* coverage Θ_{tot} (Ref. 19). Results are shown in Fig. 2. At lower fluxes, a power-law $N \propto F^{\chi}$ dependence with $\chi_{680} = 0.76 \pm 0.03, \chi_{770} = 0.75 \pm 0.04$ is observed. In the experiment, disordered growth occurred at high fluxes. In the model, deviations from the power-law behavior of $N = N(F)$ are observed.

To the best of our knowledge, our KMC model is the first one to provide scaling exponents χ close to 1. We can explain this by comparing its kinetics to the kinetics of the standard growth model obtained by ''switching off'' the barrier to attachment. The model then reduces to a variant of the standard model, with the hopping frequency of (any) HUC equal to $\nu_D = \nu_0 \exp(-E_D/k_BT)$ where $E_D = E_S + nE_N$ with n being the number of nearest-neighbor HUC's, $E_N \equiv E_N^T = 0.3$ eV the nearest-neighbor bond strength, and $E_S = 1.5$ eV the surface barrier to diffusion. We observe ''standard'' behavior[2,3] with a significantly lower scaling exponent, $\chi \approx 0.4$.

The two models differ in the evolution of the island density N as a function of coverage Θ [Figs. 3(a) and 3(b). The $N(F)$ points used in determining χ from Eq. (1) are marked ● in Figs. 3(a) and 3(b).] $N(\Theta)$ in the model without the barrier to attachment [Fig. 3(a)] evolves according to predictions of analytical models: It reaches a broad maximum and then decreases slowly due to the onset of coalescence at higher Θ. The evolution of the number of transformed islands vs coverage for the model of Si homoepitaxy is different from the evolution in the standard model [Fig. 3(b)]: The maxima are reached at higher Θ compared to the standard model, and there are no significant plateaus observed.

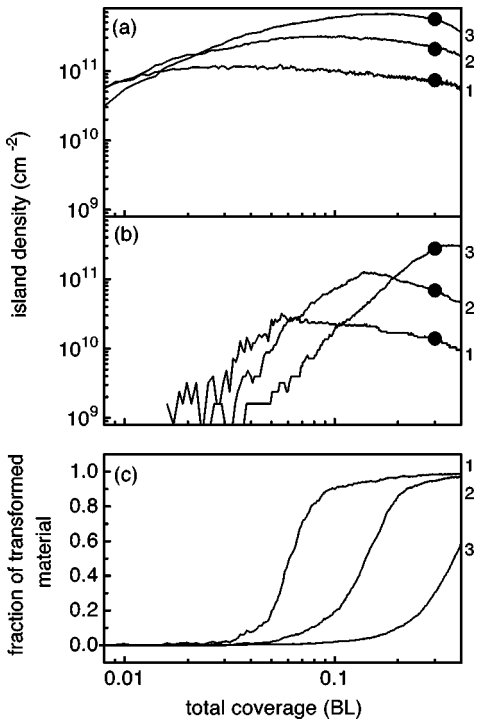

FIG. 3. Evolution of the island density vs total coverage for a model with the barriers to attachment depends on flux (b) and differs from that of a standard growth model (a). In (a) and (b), the points that contribute to the $N(F)$ curves for determination of χ in Eq. (1) are marked (●). The barrier to attachment limits the rate of creation of reconstructed islands. At high fluxes, most of the material present at the surface is nontransformed (c). Data for (1) $F=10^{-4}$ BL s^{-1}, (2) $F=10^{-3}$ BL s^{-1}, and (3) $F=10^{-2}$ BL s^{-1} are shown.

The presence of the barrier to attachment explains the shift of the maxima and the rapid increase of N with Θ. Growth of a transformed island in the model starts with transformation of three neighboring X HUC's. This happens after a certain time τ_{del} during which X HUC's are placed next to each other. This time does *not* depend on the deposition rate but instead on the strength of the barrier to attachment. The transformation becomes the rate-limiting process of island formation. The transformation onset is delayed by τ_{del} (or $\Theta_{\mathrm{del}}=F\tau_{\mathrm{del}}$) from the time when sufficient amount of material was deposited to establish X HUC trimers population (cf. Fig. 4). After τ_{del}, many transformation events take place during a short time interval, which results in a steep ''take off'' of N. By the time the transformation begins,

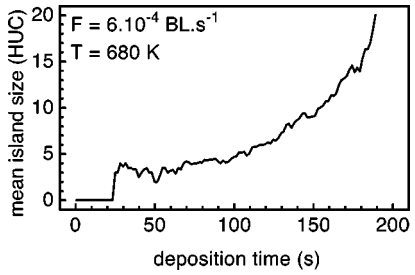

FIG. 4. The delay in island creation is clearly visible in the record of time evolution of the mean island size. Instability of newborn islands causes the decrease of $\langle s\rangle$ at short times.

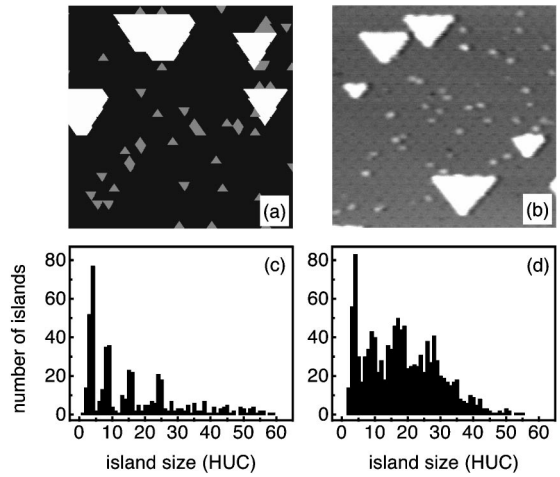

FIG. 5. Growth morphologies in the model (a) and experiment (b). During growth, magic island sizes are stabilized, resulting in a nontrivial island size distribution (c,d), Ref. 7.

more material has been deposited for a higher flux F. Therefore, the amount of nontransformed material at a given Θ_{tot} increases with increasing F [Fig. 3(c)], and so does the disorder of the quenched sample.

After reaching maximum, the decrease of the island density N in the model of Si growth is faster in comparison with the standard model. Two mechanisms may contribute to this. First, newborn islands of size 3 are unstable, and many of them decay soon after being formed (cf. Fig. 4). Therefore, the population of these islands decreases at later stages of growth when most of material deposited on the surface is captured by bigger islands. Second, due to the barrier to attachment, the capture zones around islands are missing (the islands do not ''feel'' each other). The distribution of islands over the surface is thus random (cf. Figs. 1 and 2 in Ref. 20) and coalescence starts at lower Θ as compared to the standard model.

Let us stress that the presence of the barrier to attachment and the instability of growing islands are important for obtaining high χ. With the barrier to attachment decreasing and/or the nearest-neighbor bond strength increasing, χ decreases.

The instability of growing islands does not strongly affect morphologies obtained for Si/Si(111)7×7 MBE growth. We observe the characteristic multiple-peaked island size distribution [Figs. 5(c) and 5(d)], but with broader peaks (in better agreement with the experimental results) as compared to the model with detachment of material from islands forbidden.[7] In the morphologies of experimental samples, nontransformed clusters of Si adatoms formed during quenching of samples are visible [Fig. 5(b)]. The density of nontransformed material may be experimentally determined and compared to the model results.

Analytical theories usually relate the value of the scaling exponent χ to i^*, the number of material units in a ''critical'' (i.e., largest unstable) island in the growth system. For the determination of i^*, we can use a formula $\chi=2i^*/(i^*+3)$ derived by Kandel.[5] The exponent χ in the model varies smoothly with E_S, E_N^X, and E_N^T so that the corresponding values of i^* are noninteger numbers between $i^*=1$ ($\chi=0.5$) and $i^*=2$ ($\chi=0.8$). In addition, a dependence of the

island density on E_S (the substrate contribution to the hopping barrier) was found, in contrast to predictions of Ref. 6.

Equilibration. Using scanning tunneling microscopy (STM) at an elevated temperature, the authors of Refs. 12 and 13 followed a number of isolated (a nearest island or a step edge at a distance more than 800 Å) adatom (A) or vacancy (V) islands and studied the temperature dependence of their decay rates. The decay rates ν^A, ν^V showed Arrhenius behavior $\nu^{A,V}=\nu_0^{A,V}\exp(-E_a^{A,V}/k_BT)$ with $\nu_0^A=2\times10^{11\pm1}$ adatoms s^{-1}, $E_a^A=1.5\pm0.1$ eV for adatoms, $\nu_0^V=3\times10^{9\pm1}$ adatoms s^{-1}, $E_a^V=1.3\pm0.2$ eV for vacancies, respectively. The decay rate of vacancy islands was found to be approximately 5 times lower than that of adatom islands.[21]

The authors of Refs. 12 and 13 attributed the difference between the decay rates of adatom and vacancy islands to the effect of the Ehrlich-Schwoebel (step-edge) barrier in the Si/Si(111)7×7 system. We do not believe that the Ehrlich-Schwoebel barrier plays any role here: Growth experiments provide no compelling evidence of the presence of an appreciable Ehrlich-Schwoebel barrier at step edges on Si/Si(111)7×7 surface within the relevant temperature range.[10]

With our model, we traced the evolution of a 96-HUC compact adatom or vacancy island placed on a vicinal Si surface (U-type steps, the terrace width of 480 nm, the distance from the descending step edge of 240 nm) equilibrated at a given temperature. Step edges on the vicinal surface form adatom sources and traps necessary for true disappearance of a single adatom or vacancy island in a model with periodic boundary conditions.

The temperature dependence of the decay rates for adatom and vacancy islands in our model is shown in Figs. 6(a) and 6(b). With the parameters listed above, the decay rates in the model are higher than the experimental ones ($\nu_0^A=10^{15\pm1}$ adatoms s^{-1}, $E_a^A=2.1\pm0.1$ eV, $\nu_0^V=10^{14\pm1}$ adatoms s^{-1}, $E_a^V=2.0\pm0.1$ eV), and the decay rate of vacancy islands is approximately 2 times lower than the decay rate of adatom islands.

In order to estimate the effect of the barrier to attachment on the observed differences between adatom- and vacancy-island decay, we also modeled adatom- and vacancy-islands decay with the barrier to attachment ''switched off.'' The decay rates thus obtained were lower ($\nu_0^A\approx\nu_0^V=10^{13\pm1}$ adatoms s^{-1}, $E_a^A\approx E_a^V=1.9\pm0.1$ eV), but the decay rate of vacancy islands was still approximately 2 times lower than for adatom islands. This observation agrees with results of a standard growth model on square lattice.[22] The difference between adatom- and vacancy-island decay rates on the vicinal surface thus seems to originate from the difference of geometry of adatom- and vacancy-island boundaries.[22]

In Fig. 6(c), a typical time evolution of the size of a decaying island in a model with the barriers to attachment is shown. We see that stable (''magic'') Si islands do exist. They correspond to equilibrium island shapes experimentally observed[12–14] and differ from magic shapes observed during Si/Si(111)7×7 growth.[7] Magic islands are compact (2 nearest-neighbors for all perimeter HUC's) and the barrier to attachment prevents their shape from ''being spoiled'' by attachment of material surrounding the island. No stable shapes are observed during island decay for the model without the barriers to attachment.

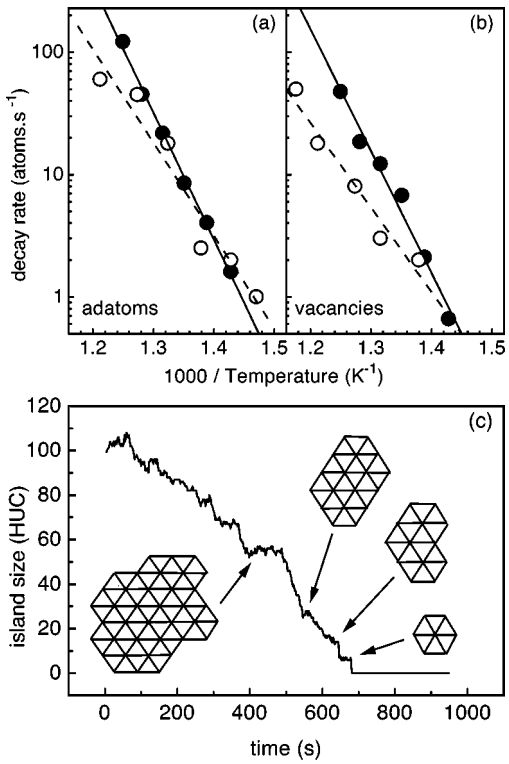

FIG. 6. Arrhenius plots of experimental (○) (Ref. 12) and modeled (●) decay rates for adatom (a) and vacancy (b) islands. In the model, the rate of a vacancy island filling is approximately $2\times$ lower than the rate of an adatom-island decay. During the island decay, ''magic'' island sizes are stabilized (c). Insets show some of the observed stable island morphologies. These are close to equilibrium island shapes (Refs. 12–14) and differ from ''magic'' island shapes observed during growth [cf. Fig. 5(b)].

In this work, we presented a coarse-grained model of Si/Si(111)7×7 MBE growth with an activation barrier to attachment of material to existing islands implemented. We demonstrated that this barrier contributes to the steep growth-rate dependence of the island density observed in Si/Si(111)7×7 MBE and helps to stabilize ''magic'' island shapes in both growth and relaxation experiments.

This work was supported by the Grant Agency of the Czech Republic, Project No. GACR 202/97/1109, and by the Volkswagen Stiftung.

*Author to whom correspondence should be addressed. Electronic address: myslivec@plasma.troja.mff.cuni.cz

[1] J. A. Venables, G. D. T. Spiller, and M. Hanbücken, Rep. Prog. Phys. **47**, 399 (1984).

[2] C. Ratsch, A. Zangwill, P. Šmilauer, and D. D. Vvedensky, Phys. Rev. Lett. **72**, 3194 (1994); Surf. Sci. Lett. **329**, L599 (1995).

[3] P.A. Mulheran and J.A. Blackman, Philos. Mag. Lett. **72**, 55 (1995); M.C. Bartelt and J.W. Evans, Phys. Rev. B **54**, R17 359 (1996).

[4] H. Tochihara and W. Shimada, Surf. Sci. **296**, 186 (1993).

[5] D. Kandel, Phys. Rev. Lett. **78**, 499 (1997).
[6] F. Thibaudau, Surf. Sci. Lett. **416**, L1118 (1998).
[7] B. Voigtländer, M. Kästner, and P. Šmilauer, Phys. Rev. Lett. **81**, 858 (1998).
[8] B. Voigtländer and T. Weber, Phys. Rev. B **54**, 7709 (1996).
[9] B. Voigtländer and T. Weber, Phys. Rev. Lett. **77**, 3861 (1996).
[10] B. Voigtländer, A. Zinner, T. Weber, and H. P. Bonzel, Phys. Rev. B **51**, 7583 (1995).
[11] L. Andersohn, Th. Berke, U. Köhler, and B. Voigtländer, J. Vac. Sci. Technol. A **14**, 312 (1996).
[12] A. Ichimiya, Y. Tanaka, and K. Ishiyama, Phys. Rev. Lett. **76**, 4721 (1996).
[13] A. Ichimiya, Y. Tanaka, and K. Hayashi, Surf. Sci. **386**, 182 (1997).
[14] U. Köhler, L. Andersohn, and B. Dahlheimer, Appl. Phys. A: Solids Surf. **57**, 491 (1993).
[15] K. Takayanagi, Y. Tanishiro, M. Takahashi, and S. Takahashi, J. Vac. Sci. Technol. A **3**, 1502 (1985).
[16] I.-S. Hwang, M.-S. Ho, and T.T. Tsong, Phys. Rev. Lett. **83**, 120 (1999).
[17] ''*In vivo*'' record of Si/Si(111)7×7 MBE is presented at http://www.fz-juelich.de/video/voigtlaender/
[18] The model is *de facto* a two-species one.
[19] The exponent χ depends on the way N in Eq. (1) is determined. For our model, both N at constant *transformed* coverage Θ_{trans} and $N=N_{\mathrm{max}}(\Theta_{\mathrm{tot}})$ give a systematically lower χ.
[20] D. Kandel and E. Kaxiras, Phys. Rev. Lett. **75**, 2742 (1995).
[21] The difference in the adatom and vacancy island decay rates (Ref. 13) resulted from a correction of raw data for STM tip effects. Without this correction, the decay rates were equal within the experimental error: $\nu_0^A=2\times10^{10\pm1}$ adatoms s^{-1}, $E_a^A=1.3\pm0.1$ eV, $\nu_0^V=4\times10^{9\pm1}$ adatoms s^{-1}, $E_A^V=1.2\pm0.2$ eV.
[22] A. Natori, M. Murayama, D. Matsumoto, and H. Yasunaga, Surf. Sci. **409**, 160 (1998).